

UC Davis

UC Davis Previously Published Works

Title

Ryanodine Receptor Type 2: A Molecular Target for Dichlorodiphenyltrichloroethane- and Dichlorodiphenyldichloroethylene-Mediated Cardiotoxicity

Permalink

<https://escholarship.org/uc/item/3492s87v>

Journal

Toxicological Sciences, 178(1)

ISSN

1096-6080

Authors

Truong, Kim M

Feng, Wei

Pessah, Isaac N

Publication Date


2020-11-01

DOI

10.1093/toxsci/kfaa139

Peer reviewed

# Ryanodine Receptor Type 2: A Molecular Target for Dichlorodiphenyltrichloroethane- and Dichlorodiphenyldichloroethylene-Mediated Cardiotoxicity

Kim M. Truong,\* Wei Feng,\* Isaac N. Pessah \*,<sup>1</sup>

\*Department of Molecular Biosciences, School of Veterinary Medicine, University of California, Davis, California 95616-5270

<sup>1</sup>To whom correspondence should be addressed at Department of Molecular Biosciences, School of Veterinary Medicine, University of California, 1089 Veterinary Medicine Drive, Davis, CA 95616. E-mail: inpessah@ucdavis.edu

## ABSTRACT

Dichlorodiphenyltrichloroethane (DDT) and its metabolite dichlorodiphenyl-dichloroethylene (DDE) are ubiquitously found in the environment and linked to cardiovascular diseases—with a majority of the work focused on hypertension. Studies investigating whether DDx can interact with molecular targets on cardiac tissue to directly affect cardiac function are lacking. Therefore, we investigated whether *o,p'*-DDT, *p,p'*-DDT, *o,p'*-DDE, or *p,p'*-DDE (DDx, collectively) can directly alter the function of human-induced pluripotent stem cell-derived cardiomyocytes (hiPSC-CMs) by assessing their effect(s) on hiPSC-CMs Ca<sup>2+</sup> dynamics. DDx (0.1–10 μM) affected hiPSC-CMs synchronous Ca<sup>2+</sup> oscillation frequency in a concentration-dependent manner, with *p,p'*-DDT and *p,p'*-DDE also decreasing Ca<sup>2+</sup> stores. HEK-RyR2 cells cultured under antibiotic selection to induce expression of wild-type mouse ryanodine receptor type 2 (RyR2) are used to further investigate whether DDx alters hiPSC-CMs Ca<sup>2+</sup> dynamics through engagement with RyR2, a protein critical for cardiac muscle excitation-contraction coupling (ECC). Acute treatment with 10 μM DDx failed to induce Ca<sup>2+</sup> release in HEK293-RyR2, whereas pretreatment with DDx (0.1–10 μM) for 12- or 24-h significantly decreased sarcoplasmic reticulum Ca<sup>2+</sup> stores in HEK-RyR2 cells challenged with caffeine (1 mM), an RyR agonist. [<sup>3</sup>H]ryanodine-binding analysis using murine cardiac RyR2 homogenates further confirmed that all DDx isomers (10 μM) can directly engage with RyR2 to favor an open (leaky) confirmation, whereas only the DDT isomers (10 μM) modestly (≤10%) inhibited SERCA2a activity. The data demonstrate that DDx increases heart rate and depletes Ca<sup>2+</sup> stores in human cardiomyocytes through a mechanism that impairs RyR2 function and Ca<sup>2+</sup> dynamics.

**Impact Statement:** DDT/DDE interactions with RyR2 alter cardiomyocyte Ca<sup>2+</sup> dynamics that may contribute to adverse cardiovascular outcomes associated with exposures.

**Key words:** DDT; DDE; organochlorines; cardiovascular disease; ryanodine receptor; human iPSC-derived cardiomyocytes.

The production and use of the organochlorine pesticide dichlorodiphenyltrichloroethane (DDT) have been banned globally since the early 1970s, except in geographical areas where vector-borne disease(s) pose a significant threat. DDT and its metabolites remain detectable in the environment and in

human tissue and serum samples (EPA, 2017; van den Berg et al., 2017; Wattigney et al., 2019; Zhu et al., 2019). Epidemiological evidence links exposure to DDT and its metabolite dichlorodiphenyldichloroethylene (DDE) to an increased risk for development of cardiovascular diseases (CVDs) (La Merrill et al., 2013; Teixeira

et al., 2015; Vafeiadi et al., 2015), which is accountable for approximately 31% of all deaths worldwide (WHO, 2017). Several studies have identified positive associations between exposure to DDT and DDE and hypertension (Donat-Vargas et al., 2018; La Merrill et al., 2013, 2016; Vafeiadi et al., 2015).

Although studies investigating the potential mechanism of action (MOA) by which DDT mediates CVDs and/or hypertension are scarce (La Merrill et al., 2016), studies investigating whether DDT and/or DDE can engage with molecular targets found within cardiac tissue, in particular cardiomyocytes, to affect cardiac function, are lacking. To bridge this gap in knowledge, we investigated whether DDT isomers and/or DDE isomers (*o,p'*-DDT, *p,p'*-DDT, *o,p'*-DDE, and *p,p'*-DDE; collectively referred to as DDx) (Supplementary Figure 1) affect human-induced pluripotent stem cell-derived cardiomyocytes (hiPSC-CMs) and to determine the relative contribution of the sarcoplasmic reticulum (SR)  $\text{Ca}^{2+}$  release channel, ryanodine receptor type 2 (RyR2), and the  $\text{Ca}^{2+}/\text{Mg}^{2+}$  dependent SR/ER  $\text{Ca}^{2+}$  ATPase (SERCA2a). These 2 proteins work in a dynamic but opposing manner to tightly regulate the release and re-uptake of SR  $\text{Ca}^{2+}$  in the cardiomyocyte. Impairment of either or both processes not only disrupts excitation-contraction coupling (ECC) but impacts the long-term health of the cardiovascular system and its resilience to stress (Denniss et al., 2020). hiPSC-CMs are widely used as a screening tool against cardiotoxic effects because they recapitulate the genetic, mechanical, and electrophysiological properties found in human heart tissue (Csobonyeiova et al., 2016; Grimm et al., 2015; Puppala et al., 2013; Sirenko et al., 2013b). Similar to cardiac muscle, dynamic changes in intracellular  $\text{Ca}^{2+}$  ( $[\text{Ca}^{2+}]_i$ ) levels generate synchronous  $\text{Ca}^{2+}$  oscillations (SCOs) in hiPSC-CMs, which have been extensively used as a model of contraction and relaxation. Assessment of alterations in hiPSC-CM  $\text{Ca}^{2+}$  dynamics (ie, SCOs) is a widely used method to screen for drug-induced cardiotoxicity, allowing for the detection of a wide array of cardiac problems including, but not limited to, arrhythmias, contractile dysfunction, and cellular toxicity (Burnett et al., 2019; Sinnecker et al., 2014; Sirenko et al., 2013b; Watanabe et al., 2017). Therefore, we assessed the effect(s) of DDx on hiPSC-CM  $\text{Ca}^{2+}$  transients and their  $\text{Ca}^{2+}$  stores. Our current studies confirmed that DDx does, indeed, impact both hiPSC-CMs SCO frequency and  $\text{Ca}^{2+}$  stores; thus, DDx can directly affect cardiac function. We, therefore, hypothesized that DDx alters  $\text{Ca}^{2+}$  dynamics in cardiomyocytes through engagement with the RyR2 and/or SERCA2a.

Cardiac RyR2 located in the SR membrane serves as the major  $\text{Ca}^{2+}$  release channel during systole (Bers, 2002; Wescott et al., 2016). During ECC,  $\text{Ca}^{2+}$  entry through L-type  $\text{Ca}^{2+}$  channels causes massive RyR2-mediated  $\text{Ca}^{2+}$  release from SR stores, a phenomenon termed  $\text{Ca}^{2+}$ -induced  $\text{Ca}^{2+}$  release, which leads to activation of myofilaments, and ultimately, contraction of cardiac muscle (Bers, 2002, 2004). Cardiac contractility strength and duration are dependent upon both the magnitude and the duration of the  $[\text{Ca}^{2+}]_i$  rise mediated by RyR2 activation, whereas the rapid reaccumulation of cytoplasmic  $\text{Ca}^{2+}$  to restore diastolic levels and replenish luminal calcium stores is mediated by SERCA2a activation (Bers, 2004; Eisner et al., 2017). It is well established that perturbation of either RyR2 and/or SERCA2a function can ultimately lead to cardiac dysfunction, remodeling, and/or heart disease/failure (Belevych et al., 2013; Sedej et al., 2014; Walweel et al., 2017). In addition, RyR2 dysfunction can further exacerbate pre-existing cardiovascular dysfunction such as hypertension mediated by anthropogenic pesticide DDT and its metabolite DDE, leading to heart failure

(HF) (Denniss et al., 2020). DDx-RyR2 and/or DDx-SERCA2a interaction may be a novel MOA by which DDx, a pesticide still utilized in tropical areas and ubiquitously found in the environment, can mediate cardiotoxicity.

## MATERIALS AND METHODS

**Materials.** *o,p'*-DDT ( $\geq 97.4\%$ ), *p,p'*-DDT ( $\geq 97.7\%$ ), *o,p'*-DDE ( $\geq 99.9\%$ ), and *p,p'*-DDE (100%) were obtained from AccuStandard (New Haven, Connecticut). [ $^3\text{H}$ ]Ryanodine (56.6 Ci/mmol) ([ $^3\text{H}$ ]Ry) was obtained from PerkinElmer (Bellerica, Massachusetts). Ryanodine ( $\geq 98.3\%$ ) was obtained from Tocris Bioscience (Minneapolis, Minnesota). Arsenazo III (AsIII;  $\geq 95\%$ ) was obtained from Santa Cruz Biotechnology (Dallas, Texas). Dithiothreitol (DTT;  $\geq 98\%$ ) and 0.1M calcium chloride solution were purchased from Fisher Scientific (Waltham, Massachusetts). Non-fluorescent acetoxymethyl ester (Fluo-4 AM;  $\geq 95\%$ ) was purchased from Invitrogen (Waltham, Massachusetts). Gelatin A from porcine skin (approximately 300 g Bloom), thapsigargin ( $\geq 98\%$ ), adenosine 5'-triphosphate magnesium salt ( $\geq 95\%$ ), phosphocreatine disodium salt hydrate ( $\geq 97\%$ ), cyclopiazonic acid (CPA;  $\geq 98\%$ ), 1M magnesium chloride solution, ruthenium red (RR;  $\geq 85\%$ ), caffeine ( $\geq 99\%$ ), phenylmethylsulfonyl fluoride (PMSF; 98%), leupeptin hydrochloride ( $\geq 90\%$ ), and type 1 creatine phosphokinase ( $\geq 150$  units/mg protein) were all obtained from Sigma-Aldrich (St. Louis, Missouri). Dimethyl sulfoxide (DMSO) was obtained from VWR Life Science (Radnor, Pennsylvania). The EarlyTox Cardiotoxicity Kit Explorer (Catalog #: R8210) and its 3 included reference standards (sotalol, propranolol, and isoproterenol) were purchased from Molecular Devices (Sunnyvale, California). All chemicals and kits were stored as recommended by the manufacturer.

**Animals.** All collections of mouse tissues from wild-type C57BL/6J mice (origin: The Jackson Laboratory, Bar Harbor, Maine) for the studies were conducted using protocols approved by the Institutional Animal Care and Use Committee (IACUC# 18094) at the University of California at Davis (Davis, California). All animals were maintained in a vivarium with constant temperature and humidity with a 12:12 h light-dark cycle. Animals were provided with Mouse Diet 20 (PicoLab) and autoclaved drinking water provided by UC Davis animal facility *ad libitum*.

**Crude mouse cardiac RyR2/SERCA2a homogenate preparations.** Cardiac muscle SR membranes enriched in RyR2 and SERCA2a obtained from 4- to 5-month-old individual male ( $n=8$ ) and female ( $n=7$ ) wild-type C57BL/6J mice were prepared as previously described (Feng et al., 2017). Whole cardiac tissue was flash frozen in liquid nitrogen, pulverized into a fine powder using a mortar and pestle, and suspended in ice-cold aqueous buffer (pH 7.4) containing (in mM) 300 sucrose, 10 HEPES, 10  $\mu\text{g}/\text{ml}$  leupeptin hydrochloride, 0.1 PMSF, 10 sodium fluoride (NaF), 2  $\beta$ -glycerophosphate disodium salt, 0.5 sodium orthovanadate ( $\text{Na}_3\text{VO}_4$ ), and 1.5 ethylene glycol tetraacetic acid (EGTA). The mixture was homogenized with three 15 s sequential bursts at speed 4 using a Cole-Parmer LabGEN 7b series portable homogenizer (Cole-Parmer, Vernon Hills, Illinois), and then centrifuged at 110 000  $\times g$  for 60 min at 4°C. Final pellets were resuspended in ice-cold aqueous buffer (pH 7.4) containing 300 mM sucrose and 10 mM HEPES, aliquoted, flash frozen, and stored at  $-80^\circ\text{C}$  for [ $^3\text{H}$ ]Ry-binding assays.

### Protein concentration determination

The Pierce BCA Protein Assay Kit (Catalog #: 23227) purchased from Thermo Fisher (Waltham, Massachusetts) was used to quantify protein concentration of all membrane protein preparations.

**[<sup>3</sup>H]Ry-binding analysis.** Specific [<sup>3</sup>H]Ry binding to mouse cardiac muscle homogenates were measured as previously described (Pessah et al., 2009). Briefly, murine RyR2 microsomes (100 μg/ml) were incubated with ice-cold aqueous binding buffer (pH 7.4) containing (in mM) 140 KCl, 15 NaCl, 20 HEPES, and nominal free Ca<sup>2+</sup> without EGTA buffering for binding of 5 nM [<sup>3</sup>H]Ry under equilibrium assay conditions (16 h; 25°C) and constant shaking. To investigate if the 4 congeners can stabilize the open confirmation of RyR2 and to compare efficacy across the 4 congeners, microsomes were incubated in the absence or presence of 10 μM *o,p'*-DDT, *p,p'*-DDT, *o,p'*-DDE, or *p,p'*-DDE. Non-specific binding was determined by incubating with 1000-fold (5 μM) additional unlabeled ryanodine. Bound ligand was separated from free ligand, and [<sup>3</sup>H]Ry trapped to the filter was quantified using a Beckman Coulter LS6500 spectrometer (Beckman Coulter, Indianapolis, Indiana). Membranes from 8 individual male mice and 7 individual female mice were tested (*n* = 15) with each membrane fraction run in triplicates. Specific radioligand binding in the presence of compound was normalized to percent DMSO vehicle control.

**Analysis of SERCA2a activity.** Specific activity of SERCA2a ATPase was measured using mouse (male and female combined) cardiac membranes enriched in RyR2 and SERCA2a, as described above, in the absence of vanadate. The rate of ATP hydrolysis was measured spectrophotometrically using a multienzyme assay that monitored NADH oxidation at 340 nm coupled to ATP hydrolysis/regeneration in the presence of pyruvate kinase II and lactate dehydrogenase (Feng et al., 2012). The SERCA2a-specific ATPase was defined by inclusion of specific SERCA inhibitors, thapsigargin (TG) and CPA. In detail, cardiac membrane preparation (50 μg/ml) was incubated in a cuvette containing 1500 μl buffer (143 mM KCl, 430 μM Sucrose, 7 mM MgCl<sub>2</sub>, 85 μM EGTA, 143 μM Ca<sup>2+</sup>, 1 mM phosphoenolpyruvate 7 mM HEPES pH, 7.0 (KOH), 1 mM Na<sub>2</sub>ATP, 100 nM rotenone (Cherednichenko et al., 2004), 30 μl coupling enzyme mixture (600–1000 units/ml pyruvate kinase, 900–1400 units/ml lactic dehydrogenase). The sample cuvettes contained vehicle (DMSO, 0.1%), or 10 μM of either *o,p'*-DDT, *p,p'*-DDT, *o,p'*-DDE, or *p,p'*-DDE, or 10 μM TG/100 nM CPA in the presence of cardiac membranes preincubated for 5 min at 32°C in a temperature controlled multi-sample unit on the photodiode array spectrophotometer (Agilent 8453; Agilent Technologies, California). Baselines were established for an additional 2 min prior to addition of NADH to the cuvette to initiate ATPase measurements. Three different concentrations of NADH, 300, 500, or 600 μM were tested in the replicated assay (total *n* = 6–9 with 2 independent cardiac membrane preparations) to assure coupling of NADH oxidation to ATP hydrolysis.

**Human embryonic kidney 293T (HEK293) cell lines.** HEK293 cells with stable, inducible expression of wild-type mouse RyR2 (HEK-RyR2) were kindly gifted to us from Dr. S.R. Wayne Chen (University of Calgary; Alberta, Canada) (Jiang et al. 2005). The HEK-RyR2 cells and wild-type HEK cells (HEK-Null) were maintained in Dulbecco's Modified Eagle Medium (DMEM) supplemented with 2 mM glutamine, 100 μg/ml streptomycin, 100 U/ml

penicillin, 1 mM sodium pyruvate, and 10% fetal bovine serum; all purchased from Thermo Fisher, and grown at 37°C under 5% CO<sub>2</sub>. HEK-RyR2 expressed RyR2 in a stable manner when maintained under antibiotic selection pressure (Jiang et al., 2005). Null cells were grown under the same conditions except no antibiotic was supplemented. Full media changes were performed every 48 h, and cells were passaged when they reached approximately 75% confluency. Western blot analysis and Ca<sup>2+</sup> imaging of HEK293 cell lines were performed with cells that were passaged no more than 15 times.

**Western blot analysis of HEK293 cell lines.** To verify that the HEK-RyR2 inducible cell line expressed RyR2 protein in a stable manner and the lack of the protein in the HEK-Null cell line, western blotting was performed on both cell lines as previously described (Truong et al., 2019). Cell samples were harvested, denatured, and ran on a precast 4%–15% gradient Mini-PROTEAN TGX gel (Bio-Rad). Proteins were transferred onto methanol-activated polyvinylidene difluoride (PVDF) membranes (0.45 μm pore size; Bio-Rad), blocked, and then incubated in primary antibodies diluted in blocking buffer containing 0.2% Tween-20 (vol/vol) overnight. Total RyR2 was detected using the C3-33 antibody (Abcam, Cambridge, England) at 1:200. The housekeeping protein glyceraldehyde 3-phosphate dehydrogenase (GAPDH; Millipore, Billerica, Massachusetts) was detected using an anti-GAPDH antibody diluted at 1:2500.

Primary antibodies were detected using secondary antibodies diluted in blocking buffer and 0.2% Tween 20 (vol/vol) at a dilution of 1:10 000 using either an 800 nm fluorescent-conjugated goat anti-mouse secondary (LI-COR), or a 700 nm fluorescent-conjugated goat anti-rabbit secondary (LI-COR). Membranes were imaged using an Odyssey Infrared Imager (LI-COR).

**Preparation and maintenance of hiPSC-CMs.** Cryopreserved hiPSC-CMs (iCell Cardiomyocytes<sup>2</sup>; Catalog #: CMC-100-012-001 and Lot #: CMC123321) derived from fibroblasts obtained from a 0- to 18-year-old female Caucasian donor with no known disease phenotype were purchased from Cellular Dynamics International (CDI; Madison, Wisconsin). The cells were prepared and maintained according to the protocol provided by the manufacturer and maintained at 37°C under 5% CO<sub>2</sub>. Briefly, the cells were thawed in proprietary CDI seeding medium, seeded (100 μl) onto sterile aqueous 0.1% gelatin-coated clear bottomed black-walled Falcon 96-well plates (Fisher Scientific; Waltham, Massachusetts) at a density of 5 × 10<sup>5</sup> cells/ml, incubated at 37°C under 5% CO<sub>2</sub> for 4 h before all media were replaced with proprietary CDI plating medium, and maintained in the incubator until ready to use. The entire media were changed every other day with fresh CDI maintenance medium and the syncytium of hiPSC-CMs was used for Ca<sup>2+</sup> imaging assays on days-in vitro 8 (DIV 8) as recommended by the manufacturer. All work with human cells were performed under a BUA protocol approved by UC Davis Environmental and Health Safety.

**Compound preparation for Ca<sup>2+</sup> imaging of HEK293 cells or hiPSC-CMs.** Dry DMSO was added to each DDT and DDE congener to create stock solution of 10 mM, which was further diluted to create secondary stock solutions. Ca<sup>2+</sup>-imaging assays of the acute effects of DDT or DDE on HEK-Null and HEK-RyR2 cells were performed similar to previously described (Truong et al., 2019). Stock concentrations of DDT or DDE were diluted in either DMEM supplemented with 2 mM glutamine, 100 μg/ml streptomycin, 100 U/ml penicillin, and 1 mM sodium pyruvate or DMEM containing no glucose and supplemented with 1 mM sodium



pyruvate and 10 mM galactose for imaging with HEK293 cells or hiPSC-CMs, respectively, for  $\text{Ca}^{2+}$ -imaging assays of 12- or 24-h subchronic effects. HEK293 cell lines and hiPSC-CMs were incubated with the diluted chemical at 37°C under 5%  $\text{CO}_2$  for 12- or 24-h depending on the assay. Final DMSO concentration was maintained at 0.1% (vol/vol) for all chemicals and across all treatments.

**Calcium imaging of HEK293 cells.** HEK-Null and inducible HEK-RyR2 cells (Jiang et al., 2005) were used for  $\text{Ca}^{2+}$  imaging to determine the effect of *o,p'*-DDT, *p,p'*-DDT, *o,p'*-DDE, or *p,p'*-DDE (collectively, DDx) on RyR2, similar to previously described for RyR1 (Truong et al., 2019). Briefly, untreated or DDx pretreated cells were loaded with 5  $\mu\text{M}$  Fluo-4 AM dissolved in warm Tyrode solution supplemented with 0.5 mg/ml bovine serum albumin (BSA) for 1 h at 37°C under 5%  $\text{CO}_2$ . Following, the plate of cells was washed and then transferred into the Fluorescent Imaging Plate Reader (FLIPR TETRA) platform (Molecular Devices, San Jose, California) where the cells were excited at 488 nm and  $\text{Ca}^{2+}$ -bound Fluo-4 emission in the 500 nm range was recorded. A 2 min baseline recording was established prior to addition of compound and an additional 8-10 min of readings were performed following the addition of compound. For acute DDx exposure studies, 2 min of baseline was recorded prior to exposing the cells to 10  $\mu\text{M}$  of either DDT or DDE in the absence or presence of 1 mM caffeine, and RyR agonist. For select experiments, 1 mM caffeine was added to the cells following either baseline recording or 100 s after addition of 10  $\mu\text{M}$  DDT or DDE. For subchronic DDx exposure studies, 2 min of baseline was recorded before addition of 1 mM caffeine.

**Calcium imaging of hiPSC-CMs.** Calcium flux in hiPSC-CMs was assessed using the no wash EarlyTox Cardiotoxicity Kit. After subchronic exposure (12 and 24 h) to DDT or DDE concentrations ranging from 0.1 to 10  $\mu\text{M}$  (approximately 33.6–3360 ng/g aqueous medium), all media were removed and the cells were then loaded with an equal volume of prewarmed calcium dye reagent and maintenance medium (1:1; 200  $\mu\text{l}$  final volume per well) and incubated at 37°C under 5%  $\text{CO}_2$  for approximately 2 h. Following, the plate of cells was transferred into the FLIPR TETRA platform where calcium flux was recorded at 515–575 nm following excitation of the cells at 470–495 nm. Readings were taken once every second for 10 min to determine the effect(s) of sub-chronic DDx exposure on hiPSC-CMs calcium flux. The cells were then challenged with 10 mM caffeine to determine the effect(s) of sub-chronic DDx exposure on calcium stores.

**Statistical analysis.** ScreenWorks® Peak Pro software version 3.2.0.14 (Molecular Devices) was used to analyze cellular imaging of  $\text{Ca}^{2+}$  transients to quantify (1) the amplitude and the area under the curve (AUC) mediated by caffeine in HEK293 cell lines, and (2) the frequency of calcium oscillations, the width at 10% amplitude, and the AUC mediated by caffeine in hiPSC-CMs. GraphPad Prism 8 software (La Jolla, California) was used to make comparisons using a one-way ANOVA with either a Tukey's post hoc test or a Dunnett's post hoc test ( $*p < .05$ ;  $**p < .01$ ;  $***p < .001$ ), where appropriate. All error bars represent standard deviation (SD) unless stated otherwise. Data analysis of SERCA2a ATPase activity was performed using OriginLab 9.0 (OriginLab, Massachusetts). One-way ANOVA, Tukey's post hoc test was used for mean comparisons; in cases where the *p*-value is  $< .05$ , the difference is regarded as significant. Statistical analyses used for each data set are described in the figure legends.

## RESULTS

### **DDT Isomers and DDE Isomers Alter hiPSC-CMs SCO Frequency, but Only *p,p'*-DDT and *p,p'*-DDE Decrease the SR Calcium Stores**

Although the raw values for each parameter per plate were consistent amongst the replicates, they were highly variable from plate to plate as exemplified with DMSO vehicle control (Figure 1A). Three positive controls included in the kit were used: (1) Sotalolol (25  $\mu\text{M}$ ), a racemic mixture that acts as a non-selective competitive  $\beta$ -adrenergic receptor blocker and a human ether-a-go-go-related gene (hERG) potassium channel blocker that slows heart rate and induces arrhythmia, (2) propranolol (1  $\mu\text{M}$ ), a non-selective beta-blocker that induces bradycardia, and (3) isoproterenol (0.5  $\mu\text{M}$ ), a beta-adrenergic agonist that produces tachycardia. Although the controls induced the expected effects on hiPSC-CMs SCO frequency, as observed with the traces, the statistical significance was diluted or completely removed if the measured parameter was not initially normalized to vehicle control from their respective plate before subsequent analysis for the respective drug effects (Figure 1B). Hence, all  $\text{Ca}^{2+}$  flux parameters measured in hiPSC-CMs were normalized to vehicle control in their respective plate before undergoing any statistical analysis. hiPSC-CMs were exposed to 0.1–10  $\mu\text{M}$  of DDx to determine which of the four isomers directly affect  $\text{Ca}^{2+}$  dynamics in cardiomyocytes. SCOs generated by the spontaneously beating hiPSC-CMs were monitored using a fluorescent imaging plate reader platform, the FLIPR TETRA, in combination with the no wash EarlyTox Cardiotoxicity Kit, which provides a  $\text{Ca}^{2+}$  sensitive indicator in combination with a proprietary masking agent that allows for mix-and-read procedures using hiPSC-CMs. Acute exposure to 10  $\mu\text{M}$  DDx did not affect hiPSC-CMs SCO (data not shown). Therefore, hiPSC-CMs were pre-exposed to DDx for 12 h before they were imaged to investigate if DDx requires time to penetrate the cell membrane to reach an intracellular target.

Pre-exposure of hiPSC-CMs to an increasing concentration of DDx (0.1–10  $\mu\text{M}$ ) for 12 h prior to SCO measurement significantly increased hiPSC-CM SCO frequency in a concentration-dependent manner. At the lowest concentration (0.1  $\mu\text{M}$ ), all DDx, with the exception of *p,p'*-DDE, significantly increased SCO frequency ( $\geq 10\%$ ) compared with DMSO vehicle control (Figs. 2A–E). Although DDx typically increased hiPSC-CMs SCO frequency in a concentration-dependent manner, 10  $\mu\text{M}$  *p,p'*-DDT or *p,p'*-DDE had the same effect as vehicle control (Figs. 2A–E). All of the DDx congeners tested tended to decrease the width of SCO, measured at 10% amplitude compared with the DMSO vehicle control, but this effect was not statistically significant (Figs. 2A–E).

The syncytium of hiPSC-CMs was also challenged with 10 mM caffeine and the AUC post-activation was analyzed to determine whether DDx affected SR calcium stores (Figs. 3A–E). SR  $\text{Ca}^{2+}$  stores in hiPSC-CMs pretreated with *o,p'*-DDT or *o,p'*-DDE were insignificantly lower than DMSO control-treated cells across all concentrations (Figs. 3A, 3B, and 3D). Although 0.1  $\mu\text{M}$  *p,p'*-DDT significantly decreased SR  $\text{Ca}^{2+}$  stores (11% lower than DMSO vehicle control), increasing the concentration of *p,p'*-DDT restored SR  $\text{Ca}^{2+}$  concentration, with 10  $\mu\text{M}$  *p,p'*-DDT re-establishing SR  $\text{Ca}^{2+}$  concentration back to the same level as DMSO vehicle control (Figure 3C). In contrast, at low  $\mu\text{M}$ -concentrations *p,p'*-DDE had no effect on  $\text{Ca}^{2+}$  release from SR stores compared with DMSO vehicle control, but diminished SR  $\text{Ca}^{2+}$  stores in a concentration-dependent fashion, with 5 and 10  $\mu\text{M}$  significantly decreasing SR  $\text{Ca}^{2+}$  stores approximately 10% below DMSO vehicle control (Figure 3E). Overall, the 2 para-chloro-substituted DDx derivatives affected SR  $\text{Ca}^{2+}$

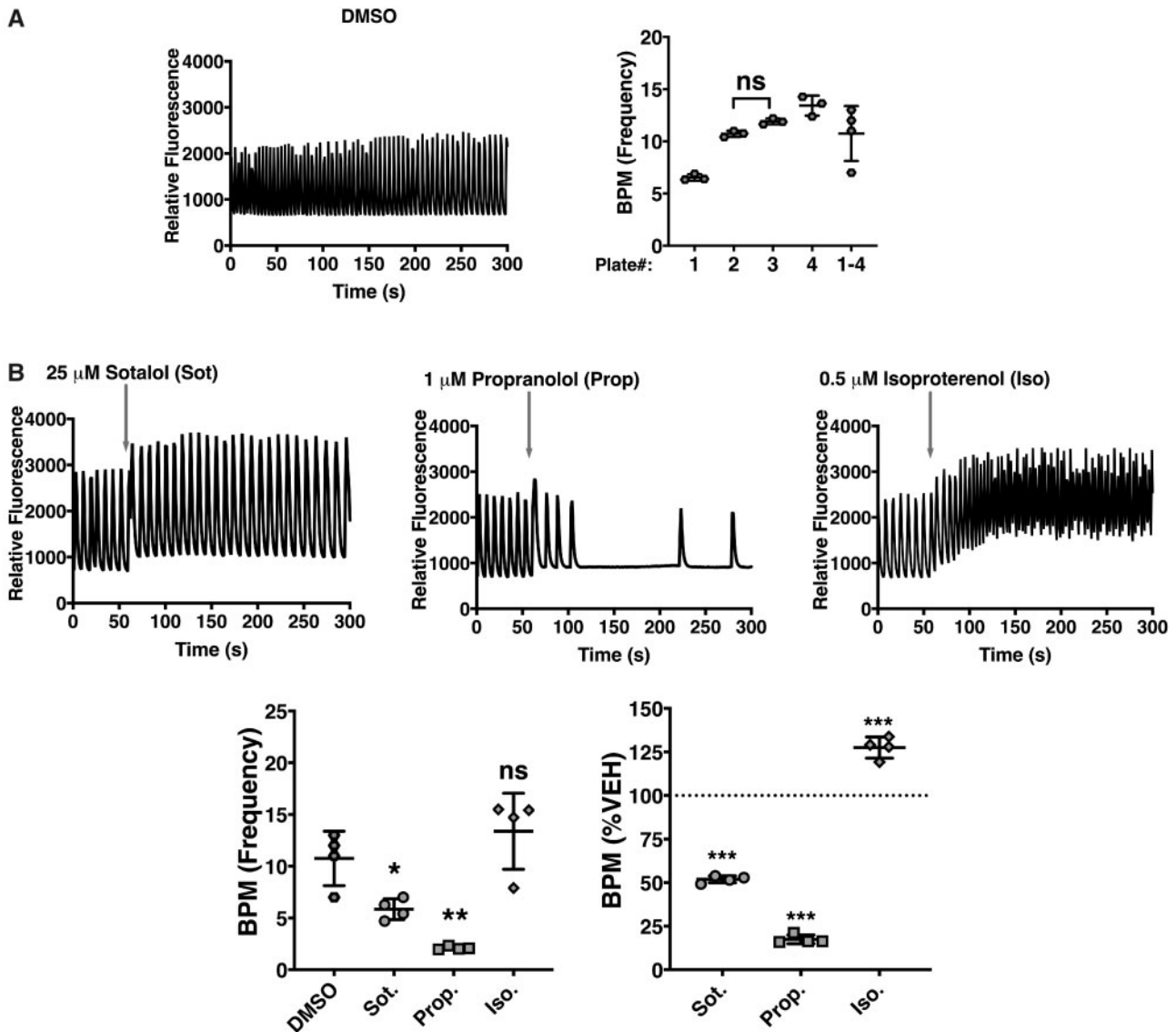


**Figure 1.** Validation and normalization of hiPSC-CMs calcium flux measurements to their respective DMSO vehicle control to correct for plate-to-plate variability. (A) Calcium transient traces of hiPSC-CMs pre-exposed to DMSO for 12 h were assessed and the frequency or beats per minute (BPM) were quantified per plate. Each individual point ( $n=3$ ) represents a replicate within the plate, whereas, each of the 4 points plotted for plate 1–4 represents the average value per individual plate. Statistical comparison of BPM amongst the different plates was performed using a one-way ANOVA with Tukey's post hoc test. Note on left panel: All values between plates were significantly different from one another except where denoted ns. (B) Calcium transient traces of hiPSC-CMs treated with either sotalol (Sot; beta-adrenergic blocker and hERG blocker), propranolol (Prop; non-selective beta-blocker), or isoproterenol (Iso; beta-adrenergic agonist)—all three serving as positive controls—were assessed and the BPM was quantified by either comparing the raw BPM value to DMSO control across all four plates, or by normalizing values to their respective DMSO control. Statistical comparison of BPM (raw value or value obtained by normalization to vehicle control) mediated by the positive controls compared with DMSO vehicle control was performed using a one-way ANOVA with a Dunnett's post hoc test ( $p < .05$ ;  $**p < .01$ ;  $***p < .001$ ). All experiments were performed in triplicate and repeated four times ( $n=4$ ).

stores more significantly than their ortho-chloro-substituted counterparts.

#### DDT and DDE Isomers Deplete Calcium Stores in HEK-RyR2 Cells

To determine whether the DDx-mediated effects on hiPSC-CMs were facilitated by interaction of DDx with RyR2, we exposed HEK293 with stable, inducible expression of mouse wild-type RyR2 receptors (HEK-RyR2) (Jiang et al., 2005) and control HEK293 cells that do not endogenously express RyR2 (HEK-Null) to DDx in the range of 0.1–10  $\mu$ M (approximately 33.6–3360 ng/g aqueous) in the absence or presence of RyR2 agonist caffeine. Western blot analysis confirmed the expression of RyR2 protein on HEK-RyR2 cells and lack, thereof, on HEK-Null cells (Figure 4).

As observed with hiPSC-CMs, acute DDx (10  $\mu$ M) exposure, alone, did not trigger  $\text{Ca}^{2+}$  release from endoplasmic reticulum (ER) stores from either HEK-RyR2 cells or HEK-Null cells (data not shown).

To determine whether DDx sensitizes RyR2 to activation by a known agonist, HEK-RyR2 cells and HEK-Null cells were exposed to either DMSO or 10  $\mu$ M DDx in combination with 1 mM caffeine. As expected, addition of caffeine, an RyR2 agonist, mediated  $\text{Ca}^{2+}$  release from HEK-RyR2 but not HEK-Null ER stores, further confirming the expression of functional RyR2 protein on HEK-RyR2 cells and lack, thereof, on HEK-Null cells (Figs. 5A and 5B). Simultaneous addition of the 2 compounds triggered  $\text{Ca}^{2+}$  release from HEK-RyR2 ER stores and the amplitude and the

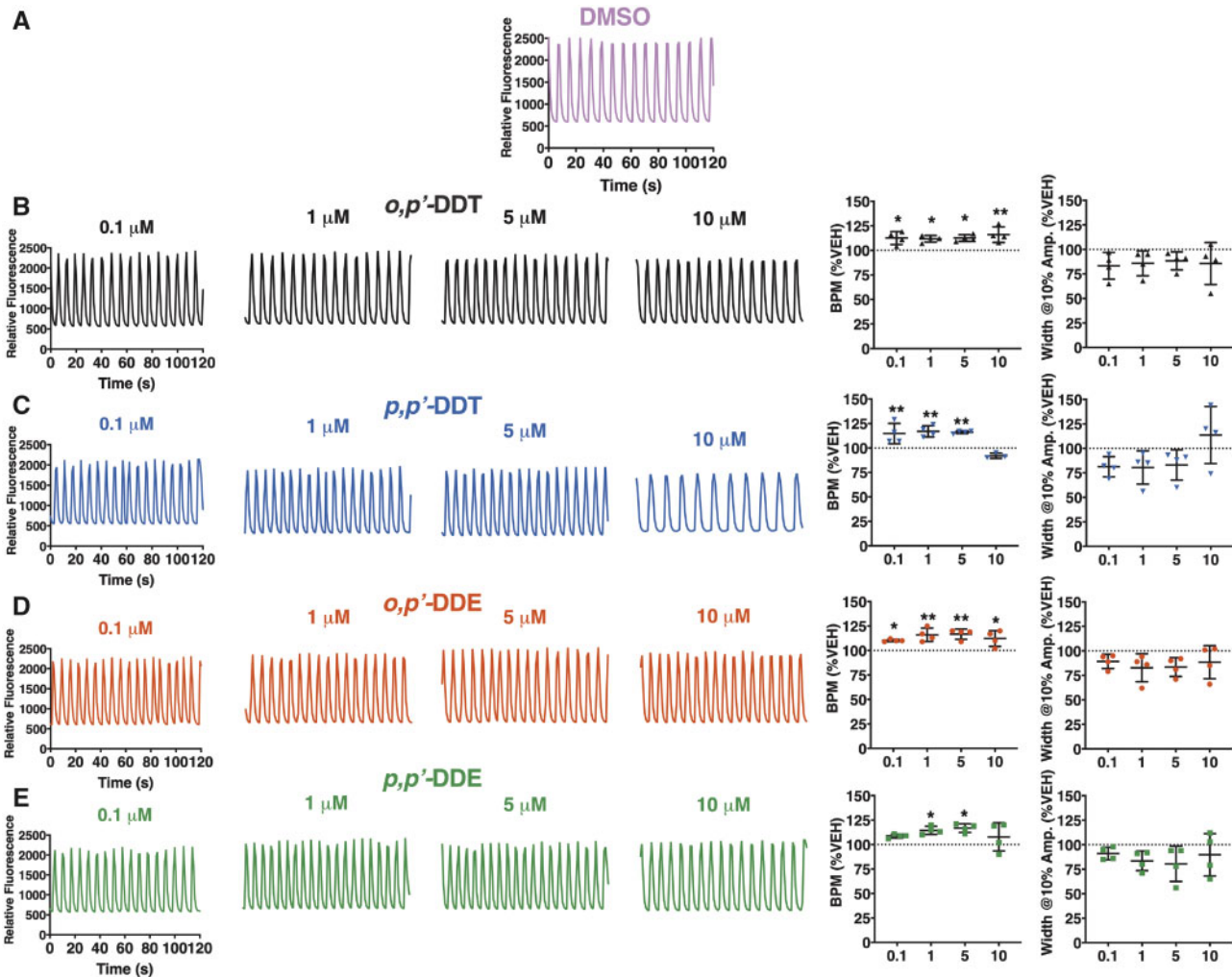


**Figure 2.** DDT and DDE isomers alter synchronous calcium oscillation (SCO) frequency in hiPSC-CMs. The BPM and the width of the calcium transients at 10% amplitude were analyzed for each hiPSC-CMs calcium transient trace pre-exposed for 12 h to (A) 0.1% DMSO (vol/vol) vehicle control (pink trace), (B) *o,p'*-DDT (black traces/inverted triangles), (C) *p,p'*-DDT (blue traces/inverted triangles), (D) *o,p'*-DDE (red traces/circles), or (E) *p,p'*-DDE (green traces/squares). All experiments were performed in triplicate and repeated four times ( $n = 4$ ). Statistical comparison of the effect of the different concentrations of DDT isomers or DDE isomers to DMSO vehicle control was performed using a one-way ANOVA with a Dunnett's post hoc test ( $*p < .05$ ;  $**p < .01$ ).

AUC of the caffeine-mediated  $\text{Ca}^{2+}$  transient in DDx-exposed cells were comparable to that of cells pretreated with DMSO (Figs. 5A, 5C, and 5E). Addition of  $10\ \mu\text{M}$  DDx 100s prior to the caffeine challenge also did not further sensitize RyR2 (Figs. 5B, 5D, and 5F).

We then posited that, similar to hiPSC-CMS, DDx requires time to penetrate the cell membrane of HEK293 cells in order to access the intracellular target. To test our hypothesis, we pre-exposed HEK293 cells with an increasing concentration of DDx ( $0.1$ – $10\ \mu\text{M}$ ) for 12 or 24 h before stimulating them with  $1\ \text{mM}$  caffeine. Pre-exposure of HEK-RyR2 cells with DDx for 12 h reduced  $\text{Ca}^{2+}$  release in a concentration-dependent manner. Cells exposed to DDT isomers or DDE isomers released significantly less  $\text{Ca}^{2+}$  from ER stores compared with DMSO vehicle control cells beginning at 5 and  $10\ \mu\text{M}$ , respectively (Figs. 6A–E). Pre-exposure of HEK-RyR2 cells for 24 h produced the same trend of diminishing  $\text{Ca}^{2+}$  release from HEK-RyR2 ER stores when exposed to caffeine, similar to what was observed with 12 h pretreatment (Figs. 7A–E).

#### *o,p'*-DDE, *p,p'*-DDE, and *o,p'*-DDT Significantly Enhance [ $^3\text{H}$ ]Ry-Binding to RyR2

Nanomolar [ $^3\text{H}$ ]Ry binds to the open conformation of RyRs, and thus, is widely used as a probe to determine (1) whether a compound directly engages with RyR, and (2) to investigate the effect of the compound on RyR conformation (Pessah and Zimanyi, 1991; Truong and Pessah, 2018; Truong et al., 2019; Zhang and Pessah, 2017). To determine which of the 4 DDx isomers directly engage with RyR2 to modulate its conformation,  $10\ \mu\text{M}$  of each isomer in combination with mouse cardiac muscle preparations were used in our [ $^3\text{H}$ ]Ry-binding assay. Cardiac preparations from individual male mice ( $n = 8$ ) and individual female mice ( $n = 7$ ) were used to increase statistical power and to investigate possible differences between sexes. No sex differences were observed (data not shown), thus all data were pooled.

Both DDE isomers and *o,p'*-DDT significantly enhanced [ $^3\text{H}$ ]Ry-binding to RyR2 (approximately 1.5 fold) compared with DMSO vehicle control, whereas *p,p'*-DDT had no significant



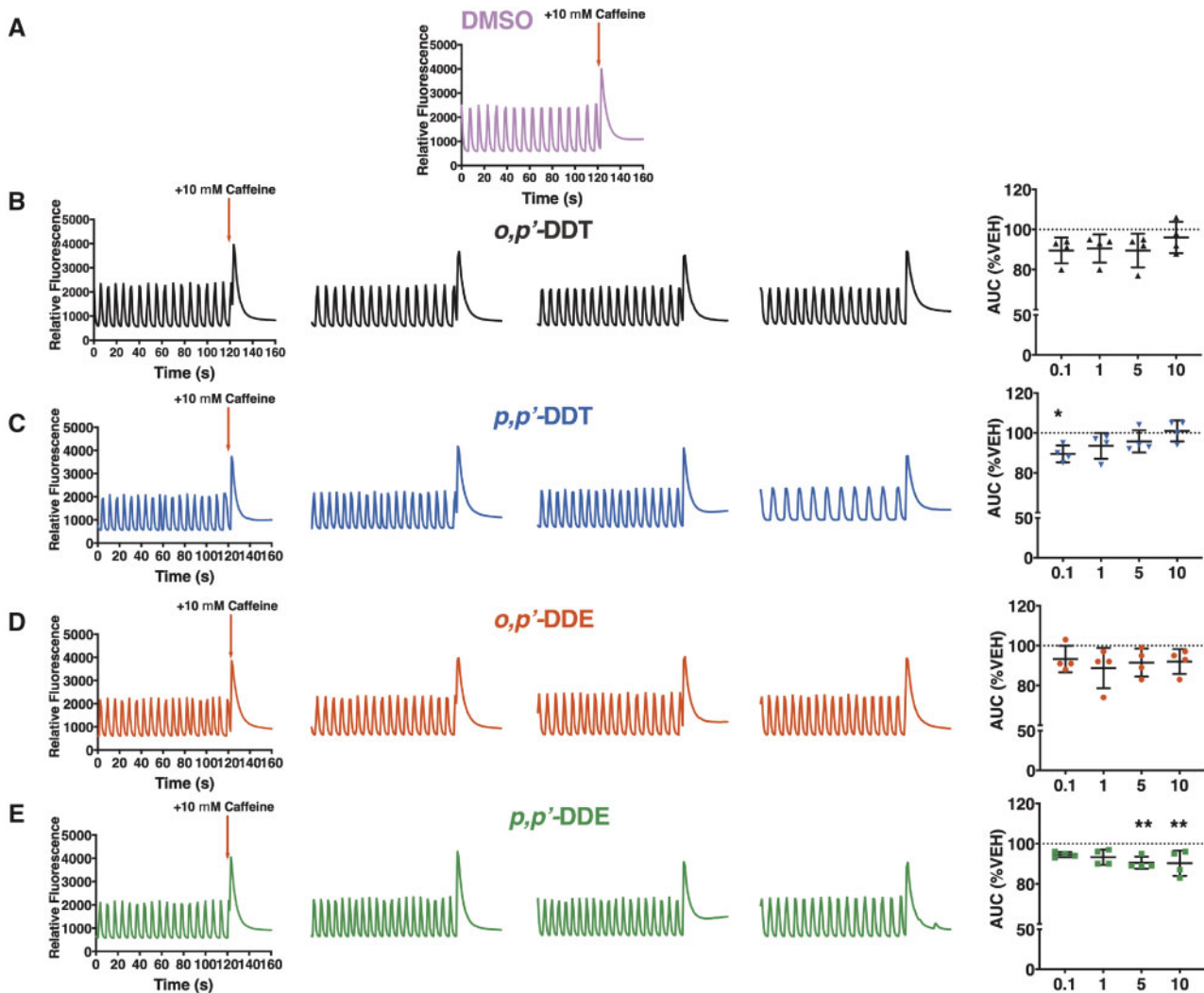


**Figure 3.** DDT and DDE isomers dampen  $\text{Ca}^{2+}$  release from SR stores in hiPSC-CMs. A 2 min baseline was recorded for hiPSC-CMs pre-exposed for 12 h to (A) 0.1% DMSO (vol/vol) vehicle control (pink trace), (B) *o,p'*-DDT (black traces/triangles), (C) *p,p'*-DDT (blue traces/inverted triangles), (D) *o,p'*-DDE (red traces/circles), or (E) *p,p'*-DDE (green traces/squares) before they were challenged with 10 mM caffeine, an RyR2 agonist. The AUC of the caffeine-mediated calcium transient was quantified, normalized to the respective vehicle control, and graphed. Experiments were performed in triplicate and repeated four times ( $n=4$ ). Statistical comparison of the different concentrations of DDT isomers or DDE isomers to DMSO vehicle control was performed using a one-way ANOVA with Dunnett's post hoc test ( $^*p < .05$ ;  $^{**}p < .01$ ).



**Figure 4.** HEK-RyR2 cells express mouse wild-type RyR2, whereas HEK-Null cells do not. Western blot analysis was performed with 15  $\mu\text{g}$  mouse cardiac muscle (positive control), HEK-Null cells (40  $\mu\text{g}$ ), and HEK-RyR2 cells (40  $\mu\text{g}$ ). GAPDH, the major housekeeping protein, was used to verify the presence of HEK-Null cells.

effect on [ $^3\text{H}$ ]Ry-binding (Figure 8). Overall, the efficacy ranking for the 4 compounds is: *o,p'*-DDE > *o,p'*-DDT > *p,p'*-DDE > *p,p'*-DDT with efficacy values significantly different between all isomers except *p,p'*-DDT and *p,p'*-DDE, which are statistically insignificant from one another (Figure 8).

#### *p,p'*-DDT and *o,p'*-DDT, But Not *p,p'*-DDE, or *o,p'*-DDE Modestly Inhibit SERCA2a

The differential influence among DDT isomers and their respective metabolites on luminal SR  $\text{Ca}^{2+}$  stores detected in cellular experiments may be the result of additional actions on SERCA2a activity. This possibility was tested using a coupled-enzyme assay to measure TG/CPA-sensitive rates of ATP hydrolysis indirectly by measuring NADH oxidation as described in Materials and Methods section. DDx ( $\leq 10 \mu\text{M}$ ) had no measurable influence on the coupling enzymes used to measure SERCA (data not shown). Figure 9 shows that preincubation of cardiac SR membranes with either 10  $\mu\text{M}$  *o,p'*-DDT or *p,p'*-DDT produced a modest (approximately 10% inhibition) of SERCA2a activity compared with vehicle control, although not statistically different from each other. In contrast, neither *o,p'*-DDE nor *p,p'*-DDE significantly depressed ATPase activity under identical assay conditions (Figure 9A). The great majority of ATPase activity measured in the cardiac membranes assayed (>90%) are inhibitable by the presence of TG/CPA (Figs. 9B and 9C, compare black and green rate lines) consistent with SERCA2a activity.



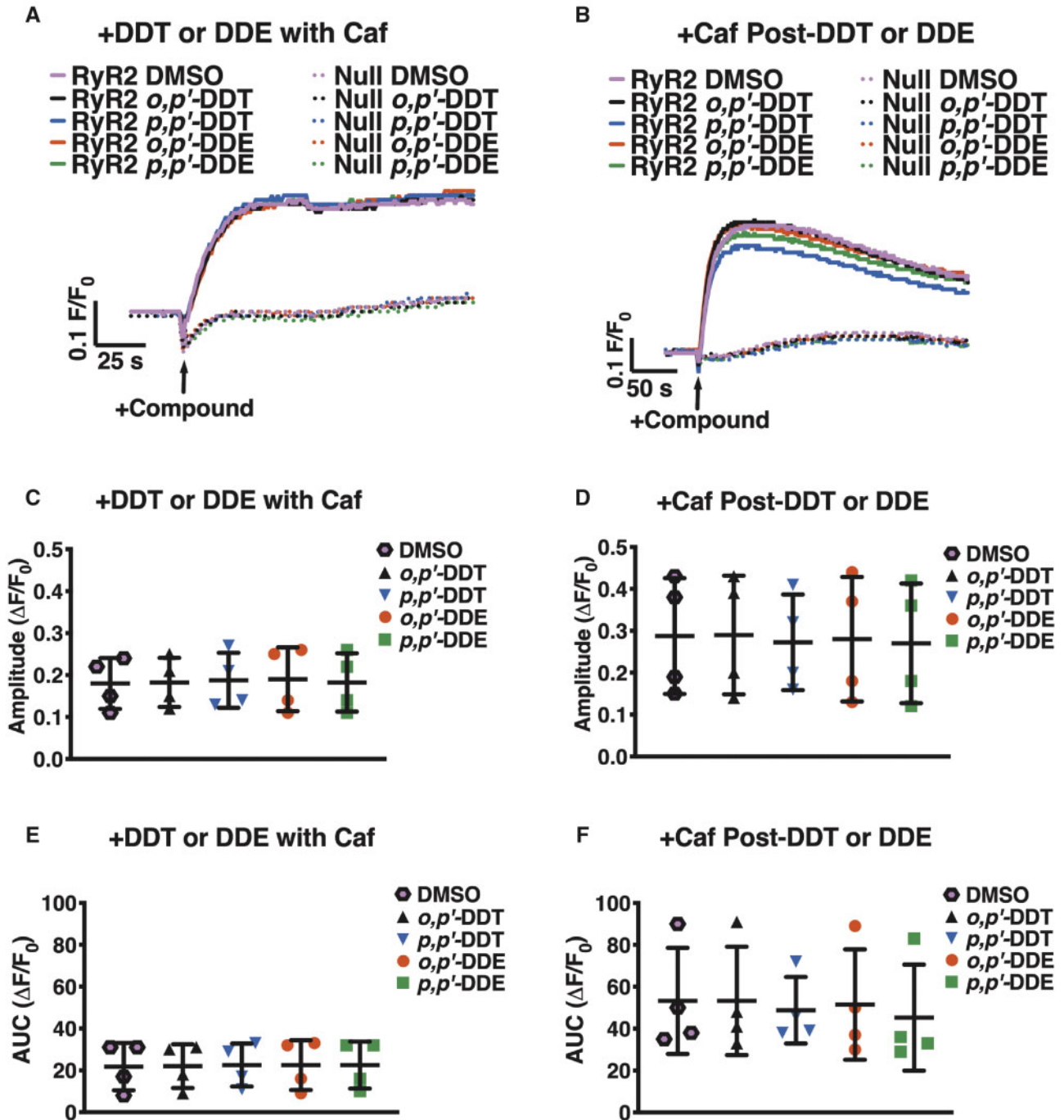
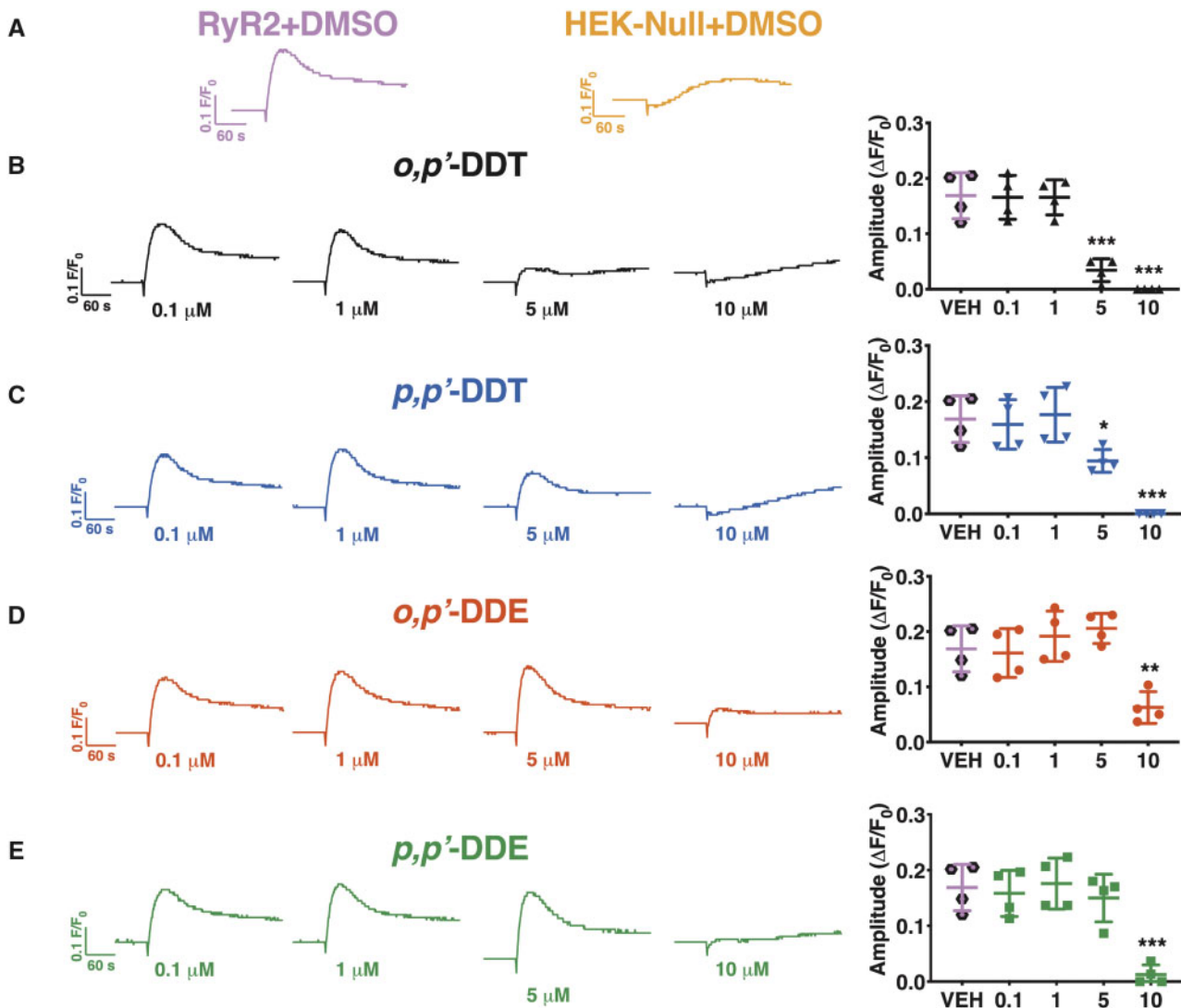


Figure 5. Acute DDT or DDE exposure does not sensitize RyR2 receptors in HEK-RyR2 cells to  $\text{Ca}^{2+}$  release. (A and B) Fluo-4 fluorescence emission traces showing  $\text{Ca}^{2+}$  transient responses of HEK-RyR2 cells and HEK-Null cells. (A) Addition of 1 mM caffeine, an RyR agonist, simultaneously with 10  $\mu\text{M}$  *o,p'*-DDT (black traces/triangles), *p,p'*-DDT (blue traces/inverted triangles), *o,p'*-DDE (red traces/circles), or *p,p'*-DDE (green traces/squares) does not sensitize RyR2 more than addition of 1 mM caffeine with 0.1% (vol/vol) DMSO vehicle (pink traces/hexagons) as assessed by the (C) amplitude and (E) AUC post-activation. (B) Addition of 10  $\mu\text{M}$  of either DDT or DDE congener 100 s before addition of 1 mM caffeine also mediated a response similar to DMSO control as assessed by the (D) amplitude and (F) AUC post-caffeine stimulation. Experiments were performed in triplicate and repeated four times ( $n=4$ ). Statistical comparison of the effect of DDT and DDE congeners to DMSO vehicle control was performed with a one-way ANOVA with Dunnett's post hoc test.

## DISCUSSION

Cross-sectional and longitudinal studies have established a positive correlation between DDx exposure and increased risk for hypertension and/or CVDs in middle-aged men and women (Cocco et al., 1997; Donat-Vargas et al., 2018; La Merrill et al., 2013;

Ljunggren et al., 2014; Vafeiadi et al., 2015). The association between DDx levels and measures of cardiac disease (eg. left ventricular mass) has been mainly attributed to obesity (La Merrill et al., 2018) rather than direct influences of DDx accumulation within heart tissues, in particular cardiac muscle. However, DDx congeners have been shown to accumulate in heart tissue of



**Figure 6.** Subchronic (12 h) DDT or DDE exposure decreases HEK-RyR2  $\text{Ca}^{2+}$  release in a concentration-dependent manner. (A)  $\text{Ca}^{2+}$  transient response mediated by addition of 1 mM caffeine to HEK-RyR2 cells (pink trace/hexagons) or HEK-Null cells (orange trace) pretreated with DMSO. HEK-RyR2 cells were pretreated for 12 h with 0.1–10  $\mu\text{M}$  (B) *o,p'*-DDT (black traces/triangles), (C) *p,p'*-DDT (blue traces/inverted triangles), (D) *o,p'*-DDE (red traces/circles), or (E) *p,p'*-DDE (green traces/squares) and challenged with 1 mM caffeine. The amplitude of the caffeine response was quantified and graphed for each concentration tested. Experiments were performed in triplicate and repeated four times ( $n = 4$ ). Statistical comparison of the effect of the different concentrations of DDT isomers or DDE isomers to DMSO vehicle control was performed using a one-way ANOVA with Dunnett's post hoc test (\*\* $p < .01$ ; \*\*\* $p < .001$ ).

wildlife, including sea turtles (Wafu et al., 2005) and vultures (van Wyk et al., 2001). Studies investigating the MOA by which DDx mediates hypertension or CVDs are lacking. In particular, to our knowledge, there are currently no studies investigating whether DDx can directly cause cardiac dysfunction through engagement with molecular targets expressed by cardiac muscle itself. Therefore, we bridged this gap in knowledge by firstly assessing the impact of DDx on hiPSC-CMs. hiPSC-CMs pre-exposed to DDx typically showed a concentration-dependent increase in SCO frequency. Since  $\text{Ca}^{2+}$  transients synchronize with cell beating, assessment of SCO frequency is utilized to determine whether a compound(s) affects heart rate (Sirenko et al., 2013a). However, it should be emphasized that interpretation of the potential *in vivo* impact of SCO frequency and their modification measured in hiPSC-CMs needs to be cautiously interpreted since these oscillations are not under control of membrane voltage. Future studies incorporating multiplexed optical sensors of membrane voltage,  $\text{Ca}^{2+}$  dynamics, and

redox status will likely further refine the observations reported here with hiPSC-CMs (Werley et al., 2020).

All four DDx isomers also decreased hiPSC-CMs SR  $\text{Ca}^{2+}$  stores, with 0.1  $\mu\text{M}$  *p,p'*-DDT and 5- and 10- $\mu\text{M}$  *p,p'*-DDE reducing  $\text{Ca}^{2+}$  stores significantly below those observed in DMSO control cells. These aforementioned actions of DDx isomers occur at concentrations well below those that inhibit SERCA2a. In fact, 10  $\mu\text{M}$  of either DDT isomer was needed to modestly inhibit ( $\leq 10\%$ ) SERCA2a, whereas the same high concentration of either DDE isomers failed to significantly depress SERCA2a activity. SR stores supply the majority of  $\text{Ca}^{2+}$  required for muscle force generation, therefore a significant depression in SR  $\text{Ca}^{2+}$  content is thought to underlie insufficient muscle force during systole, which is a contributing factor of cardiac dysfunction (Shannon et al., 2003; Walweel et al., 2017). Since DDx affected both SCO frequency and SR  $\text{Ca}^{2+}$  stores without appreciable inhibition of SERCA2a, we hypothesize that these effects are primarily mediated by DDx isomers engaging with RyR2. RyR2 is

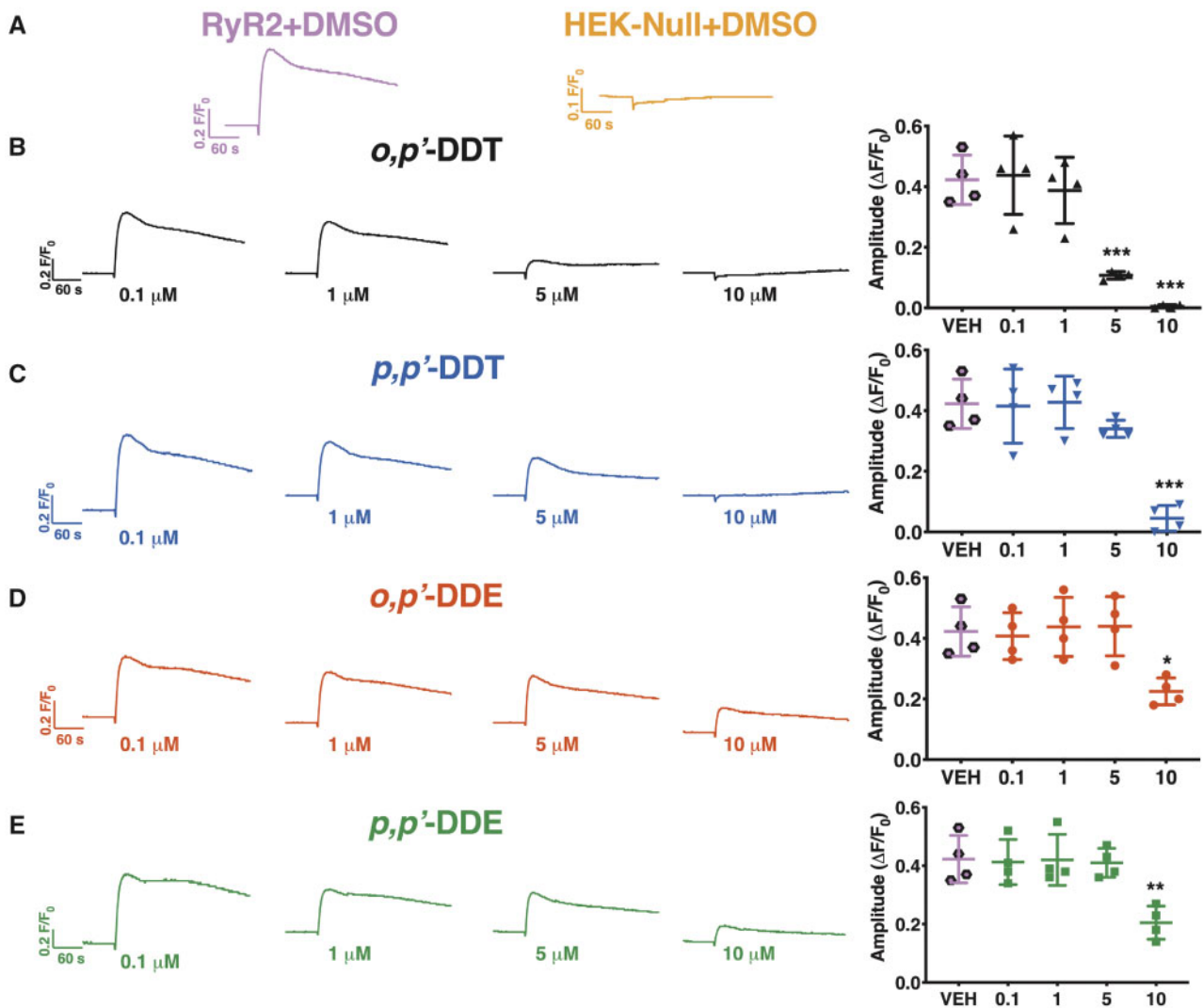


**Figure 7.** Pretreatment of HEK-RyR2 cells for 24 h with an increasing concentration of DDT or DDE has a similar effect as 12 h pretreatment. (A) Ca<sup>2+</sup> transient response mediated by addition of 1 mM caffeine to HEK-RyR2 cells (pink trace) or HEK-Null cells (orange trace) pretreated with DMSO. HEK-RyR2 cells pretreated with 0.1–10 μM (B) *o,p'*-DDT (black traces/triangles), (C) *p,p'*-DDT (blue traces/inverted triangles), (D) *o,p'*-DDE (red traces/circles), or (E) *p,p'*-DDE (green traces/squares) for 24 h and then exposed to 1 mM caffeine. The amplitude of the caffeine response was quantified and graphed for each concentration. Experiments were performed in triplicate and repeated four times ( $n=4$ ). Statistical comparison of the effect of the different concentrations of DDT isomers or DDE isomers to DMSO vehicle control was performed using a one-way ANOVA with Dunnett's post hoc test (\* $p < .05$ ; \*\* $p < .01$ ; \*\*\* $p < .001$ ).

known to play a pivotal role in determining heart rate in mammals and it is the major intracellular Ca<sup>2+</sup> release channel responsible for maintaining SR Ca<sup>2+</sup> stores (Bround et al., 2012; Yang et al., 2002). The hiPSC-CMs express RYR2 gene transcription (Puppala et al., 2013), and we observed that they respond to a caffeine challenge, confirming the presence of RyR2 and further supporting the explanation that DDx engages with RyR2 to mediate the observed alterations in hiPSC-CMs function.

Using a HEK293 cell model that expresses recombinant wild-type mouse RyR2 protein (HEK-RyR2), we demonstrated that DDx can engage with RyR2 in intact cells, although the isomers required time to penetrate the cell membrane to reach the intracellular target. HEK-RyR2 cells challenged with 1 mM caffeine after pretreatment with  $\geq 5 \mu\text{M}$  of *o,p'*-DDT or *p,p'*-DDT or 10 μM of *o,p'*-DDE or *p,p'*-DDE exhibited no Ca<sup>2+</sup> release or significantly reduced Ca<sup>2+</sup> release compared with DMSO controls. The concentration-dependent decrease in Ca<sup>2+</sup> release suggests that DDx interacts with RyR2 to diminish Ca<sup>2+</sup> stores. Whereas DDx

mediates a monotonic reduction in ER Ca<sup>2+</sup> stores in the HEK-RyR2 cell model, a non-monotonic (ie, biphasic) concentration-effect relationship is observed with hiPSC-CMs with respect to influences on SCO patterns. This is not unexpected because the two cell models (excitable vs non-excitable) regulate their intracellular Ca<sup>2+</sup> dynamics in fundamentally different ways, and may exhibit different compensatory mechanisms. For example, it has been demonstrated that hiPSC-CMs compensate for RyR2 deficiency through an IP3R-mediated mechanism, allowing for the continual generation of (abnormal) SCOs (Luo et al., 2020). Recently, DDx isomers have been demonstrated to elicit oxidative stress in myotubes (Park et al., 2020), but the consequences may be cell-type dependent. RyRs have been shown to be tightly regulated by cellular redox state in a biphasic manner (Feng et al., 1999) and could underly the biphasic responses seen of hiPSC-CMs to DDx because oxidation of RyR2 was shown to influence the threshold for SR store overload-induced Ca<sup>2+</sup> release (Waddell et al., 2016), although this needs further

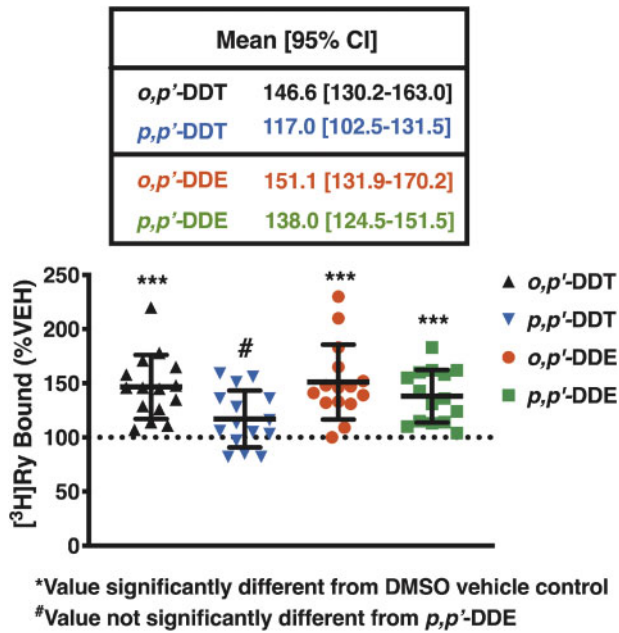


**Figure 8.** *o,p'*-DDE, *p,p'*-DDE, *o,p'*-DDT, but not *p,p'*-DDT, significantly enhance [<sup>3</sup>H]Ry binding to RyR2 compared with DMSO vehicle control. At 10 μM, *o,p'*-DDT (black triangles), *p,p'*-DDT (blue inverted triangles), *o,p'*-DDE (red circles), but not *p,p'*-DDE (green squares) increased [<sup>3</sup>H]Ry binding to mouse RyR2 approximately 1.5-fold greater than 0.1% (vol/vol) DMSO vehicle control. Efficacy was statistically different amongst all isomers except for *p,p'*-DDT and *p,p'*-DDE, which were similar. Experiments were performed in triplicate using preparations from eight individual male mice and preparations from seven individual female mice (*n* = 15). Statistical comparison of efficacy amongst all compounds was performed with a one-way ANOVA with Tukey's post hoc test (\*\**p* < .001).

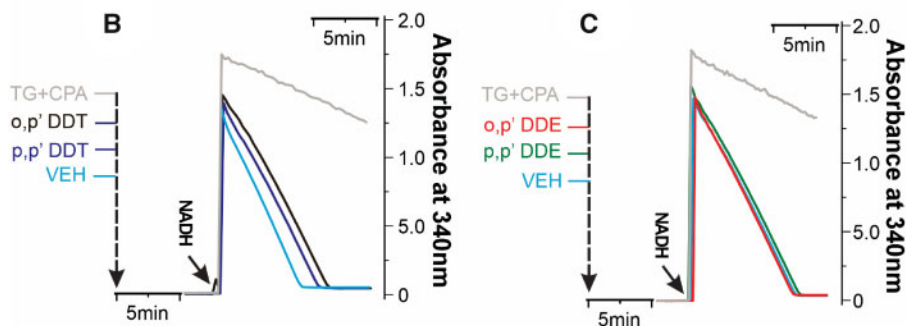
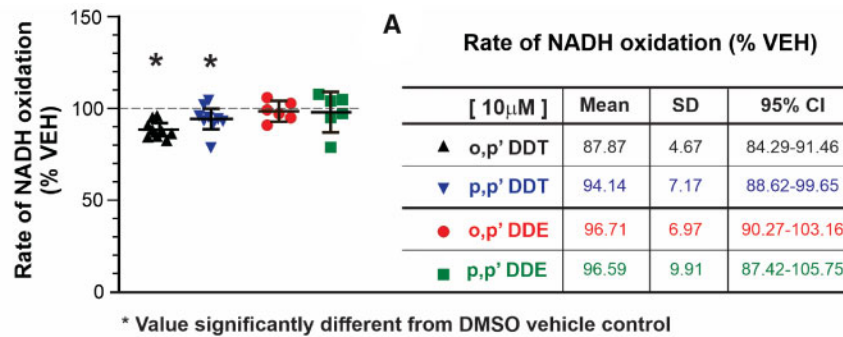


**Figure 9.** *o,p'*-DDT and *p,p'*-DDT, but not *o,p'*-DDE, or *p,p'*-DDE mildly inhibit SERCA2a. Specific SERCA2a-mediated ATP hydrolysis was monitored indirectly by measuring NADH oxidation using the coupled-enzyme assay. Thapsigargin (TG, 10 μM) and cyclopiazonic acid (CPA, 100 nM) were used to correct rates from non-SERCA mediated ATP hydrolysis. (A) NADH oxidation rates normalized to vehicle control (mean ± SD) from *n* = 6–9 replicate measurements from two independent cardiac membrane preparations from mouse heart muscles. \**p* < .05 from one-way ANOVA with Tukey's post hoc test. The table summarizes statistical parameters. Control (Vehicle) rate ranged 0.14–0.63 μM NADH/min/μg protein with 300, 500, or 600 μM NADH (see Materials and Methods section). Experimental sequence and representative raw data traces for (B) DDT and (C) DDE, when 500 μM NADH is added to start the experiment.

investigation. Nevertheless, we cannot discount other possible explanations for the observed DDx-mediated diminution in Ca<sup>2+</sup> release. For example, another potential explanation may be that DDx is affecting the SERCA pump. However, measurements of SERCA2a ATPase indicated that a high concentration (10 μM) of *o,p'*-DDT or *p,p'*-DDT mildly inhibited SERCA2a activity, whereas the DDE isomers at the same concentration had no effect. Considering SERCA2a is expressed at very high density within the SR of cardiomyocytes, this level of inhibition is unlikely to contribute appreciably to the net SR Ca<sup>2+</sup> depletion observed. This interpretation is supported by results from HEK-null cells where none of the DDx isomers elicited SR Ca<sup>2+</sup> depletion in the absence of RyR expression. Results from [<sup>3</sup>H]Ry-binding assay, where nanomolar [<sup>3</sup>H]Ry binds to the open conformation of RyR2, support a direct modulation of DDx isomers with RyR2. Whether DDx can function as a partial antagonist at lower concentrations and a full antagonist at higher concentrations to decrease RyR2 sensitivity or to promote a closed confirmation, respectively, requires further investigation.

Regardless of the exact mechanism by which DDx modulates RyR2, it is well established that perturbation of RyR2 conformation and/or function, whether mediated by a compound or due to an inherent genetic mutation, can result in cardiac dysfunction or even progression to HF (Belevych *et al.*, 2013; Walweel and Laver, 2015; Walweel *et al.*, 2017). Conversely, RyR2 dysfunction can result from hypertension-mediated HF (Messerli *et al.*, 2017; Skinner *et al.*, 2019). Although the exact MOA by which DDx facilitates hypertension is unknown, it is recognized that hypertension whether mediated by a compound or a predisposition due to genetics, can manifest into heart disease and



negatively affect cardiac health (Messerli et al., 2017). In a majority of hypertensive patients cardiac remodeling occurs, leading to cardiac hypertrophy, which is a recognized risk factor for stroke, HF, and coronary events (Aronow, 2017). RyR2 has been shown to be required for the development of pressure-overload triggered cardiac hypertrophy (Zou et al., 2011). Therefore, RyR2 can be seen as both a cause and a consequence of HF and decreased cardiac function. Since DDx can mediate hypertension, which, in turn can affect RyR2, and also directly affect RyR2, DDx poses a dual threat to cardiovascular health.

It should be noted that while RyR2-mediated  $Ca^{2+}$  leak or increased activity is observed during HF, in cases of arrhythmia, and a cause of cardiac remodeling, it does not always manifest as an abnormality in either cardiac function or structure unless challenged by a triggering agent such as exercise or stress as in the case of catecholaminergic polymorphic ventricular tachycardia (Belevych et al., 2013; Marx and Marks, 2013; Sedej et al., 2014). Hence, while current studies have linked DDx solely to hypertension, it is possible that DDx initially causes more subtle effects such as mediating RyR2 dysregulation and making it more susceptible to triggering agents, which can lead to a decline in cardiac health over time. Overall, it is critical to consider how interaction of DDx with RyR2 can weaken the cardiac system as a whole and make it more susceptible to development of a CVD or hypertension.

Additionally, it has been demonstrated that *p,p'*-DDE, through its obesogenic properties, can indirectly alter cardiac function by producing an increase in left ventricular (LV) mass and hypertrophy (La Merrill et al., 2018) with promotion of obesity also linked to development of CVDs or chronic HF (Selthofer-Relatic et al., 2019). Obesity and/or LV enlargement can lead to HF with reduced ejection fraction, which can ultimately lead to the development of musculoskeletal consequences such as cardiac cachexia, typically preceded by sarcopenia (Selthofer-Relatic et al., 2019; Sisto et al., 2018). Our laboratory previously published findings demonstrating that DDx can directly interact with skeletal muscle ryanodine receptor type 1 (RyR1) to contribute to potential long-term impairments in muscle health (Truong et al., 2019). Since DDx can disrupt ECC in both cardiac and skeletal muscle and cardiac function is not independent of skeletal muscle health, our data suggest that DDx can potentially impair muscle health by directly affecting skeletal muscle machinery and also indirectly by perturbing cardiac function.

To our knowledge, we are the first laboratory to demonstrate that DDx can directly impair calcium dynamics in cardiomyocytes, and may do so through engagement with RyR2. However, since our study investigates the interaction of DDx solely with RyR2 and SERCA2a, only two components of the macromolecular complex that regulates ECC in a normally functioning heart, future studies are necessary to determine if, and what other cardiac tissue-specific molecular targets DDx may also affect.

## SUPPLEMENTARY DATA

Supplementary data are available at Toxicological Sciences online.

## DECLARATION OF CONFLICTING INTERESTS

The authors declared no potential conflicts of interest with respect to the research, authorship, and/or publication of this article.

## FUNDING

This work was supported by the National Institute of Environmental Health Sciences [R01 ES014901, P01 AR052354, P01 ES011269, and P42 ES04699], the National Science Foundation [1840842], and the US Environmental Protection Agency [STARR829388 and R833292].

## REFERENCES

- Aronow, W. S. (2017). Hypertension and left ventricular hypertrophy. *Ann. Transl. Med.* 5, 310.
- Belevych, A. E., Radwański, P. B., Carnes, C. A., and Györke, S. (2013). 'Ryanopathy': Causes and manifestations of RyR2 dysfunction in heart failure. *Cardiovasc. Res.* 98, 240–247.
- Bers, D. M. (2002). Cardiac excitation-contraction coupling. *Nature* 415, 198–205.
- Bers, D. M. (2004). Macromolecular complexes regulating cardiac ryanodine receptor function. *J. Mol. Cell. Cardiol.* 37, 417–429.
- Bround, M. J., Asghari, P., Wambolt, R. B., Bohunek, L., Smits, C., Philit, M., Kieffer, T. J., Lakatta, E. G., Boheler, K. R., Moore, E. D. W., et al. (2012). Cardiac ryanodine receptors control heart rate and rhythmicity in adult mice. *Cardiovasc. Res.* 96, 372–380.
- Burnett, S. D., Blanchette, A. D., Grimm, F. A., House, J. S., Reif, D. M., Wright, F. A., Chiu, W. A., and Rusyn, I. (2019). Population-based toxicity screening in human induced pluripotent stem cell-derived cardiomyocytes. *Toxicol. Appl. Pharmacol.* 381, 114711.
- Cherednichenko, G., Zima, A. V., Feng, W., Schaefer, S., Blatter, L. A., and Pessah, I. N. (2004). NADH oxidase activity of rat cardiac sarcoplasmic reticulum regulates calcium-induced calcium release. *Circ. Res.* 94, 478–486.
- Cocco, P., Blair, A., Congia, P., Saba, G., Ecce, A. R., and Palmas, C. (1997). Long-term health effects of the occupational exposure to DDT. A preliminary report. *Ann. N. Y. Acad. Sci.* 837, 246–256.
- Csibonyeiova, M., Polak, S., and Danisovic, L. (2016). Toxicity testing and drug screening using iPSC-derived hepatocytes, cardiomyocytes, and neural cells. *Can. J. Physiol. Pharmacol.* 94, 687–694.
- Denniss, A. L., Dashwood, A. M., Molenaar, P., and Beard, N. A. (2020). Sarcoplasmic reticulum calcium mishandling: Central tenet in heart failure? *Biophys. Rev.* 12, 865–878.
- Donat-Vargas, C., Åkesson, A., Tornevi, A., Wennberg, M., Sommar, J., Kiviranta, H., Rantakokko, P., and Bergdahl, I. A. (2018). Persistent organochlorine pollutants in plasma, blood pressure, and hypertension in a longitudinal study. *Hypertension* 71, 1258–1268.
- Eisner, D. A., Caldwell, J. L., Kistamas, K., and Trafford, A. W. (2017). Calcium and excitation-contraction coupling in the heart. *Circ. Res.* 121, 181–195.
- EPA, ed. (2017). *DDT - A Brief History and Status*. World Health Organization, Washington, DC.
- Feng, W., Hwang, H. S., Kryshal, D. O., Yang, T., Padilla, I. T., Tiwary, A. K., Puschner, B., Pessah, I. N., and Knollmann, B. C. (2012). Coordinated regulation of murine cardiomyocyte contractility by nanomolar (-)-epigallocatechin-3-gallate, the major green tea catechin. *Mol. Pharmacol.* 82, 993–1000.
- Feng, W., Liu, G., Xia, R., Abramson, J. J., and Pessah, I. N. (1999). Site-selective modification of hyperreactive cysteines of ryanodine receptor complex by quinones. *Mol. Pharmacol.* 55, 821–831.

- Feng, W., Zheng, J., Robin, G., Dong, Y., Ichikawa, M., Inoue, Y., Mori, T., Nakano, T., and Pessah, I. N. (2017). Enantioselectivity of 2,2',3,5',6'-pentachlorobiphenyl (PCB 95) atropisomers toward ryanodine receptors (RyRs) and their influences on hippocampal neuronal networks. *Environ. Sci. Technol.* **51**, 14406–14416.
- Grimm, F. A., Iwata, Y., Sirenko, O., Bittner, M., and Rusyn, I. (2015). High-content assay multiplexing for toxicity screening in induced pluripotent stem cell-derived cardiomyocytes and hepatocytes. *Assay Drug Dev. Technol.* **13**, 529–546.
- Jiang, D., Wang, R., Xiao, B., Kong, H., Hunt, D. J., Choi, P., Zhang, L., and Chen, S. R. W. (2005). Enhanced store overload-induced Ca<sup>2+</sup> release and channel sensitivity to luminal Ca<sup>2+</sup> activation are common defects of RyR2 mutations linked to ventricular tachycardia and sudden death. *Circ. Res.* **97**, 1173–1181.
- La Merrill, M., Cirillo, P. M., Terry, M. B., Krigbaum, N. Y., Flom, J. D., and Cohn, B. A. (2013). Prenatal exposure to the pesticide DDT and hypertension diagnosed in women before age 50: A longitudinal birth cohort study. *Environ. Health Perspect.* **121**, 594–599.
- La Merrill, M. A., Lind, P. M., Salihovic, S., van Bavel, B., and Lind, L. (2018). The association between p, p'-DDE levels and left ventricular mass is mainly mediated by obesity. *Environ. Res.* **160**, 541–546.
- La Merrill, M. A., Sethi, S., Benard, L., Moshier, E., Haraldsson, B., and Buettner, C. (2016). Perinatal DDT exposure induces hypertension and cardiac hypertrophy in adult mice. *Environ. Health Perspect.* **124**, 1722–1727.
- Ljunggren, S. A., Helmfrid, I., Salihovic, S., van Bavel, B., Wingren, G., Lindahl, M., and Karlsson, H. (2014). Persistent organic pollutants distribution in lipoprotein fractions in relation to cardiovascular disease and cancer. *Environ. Int.* **65**, 93–99.
- Luo, X., Li, W., Künzel, K., Henze, S., Cyganek, L., Strano, A., Poetsch, M. S., Schubert, M., and Guan, K. (2020). IP3R-mediated compensatory mechanism for calcium handling in human induced pluripotent stem cell-derived cardiomyocytes with cardiac ryanodine receptor deficiency. *Front. Cell Dev. Biol.* **8**, 772.
- Marx, S. O., and Marks, A. R. (2013). Dysfunctional ryanodine receptors in the heart: New insights into complex cardiovascular diseases. *J. Mol. Cell. Cardiol.* **58**, 225–231.
- Messerli, F. H., Rimoldi, S. F., and Bangalore, S. (2017). The Transition From Hypertension to Heart Failure: Contemporary Update. *JACC Heart Fail.* **5**, 543–551.
- Park, C. M., Kim, K. T., and Rhyu, D. Y. (2020). Low-concentration exposure to organochlorine pesticides (OCPs) in L6 myotubes and RIN-m5F pancreatic beta cells induces disorders of glucose metabolism. *Toxicol. In Vitro* **65**, 104767.
- Pessah, I. N., Lehmler, H.-J., Robertson, L. W., Perez, C. F., Cabrales, E., Bose, D. D., and Feng, W. (2009). Enantiomeric Specificity of (–)-2,2',3,3',6,6'-Hexachlorobiphenyl toward Ryanodine Receptor Types 1 and 2. *Chem. Res. Toxicol.* **22**, 201–207.
- Pessah, I. N., and Zimanyi, I. (1991). Characterization of multiple [3H]ryanodine binding sites on the Ca<sup>2+</sup> release channel of sarcoplasmic reticulum from skeletal and cardiac muscle: Evidence for a sequential mechanism in ryanodine action. *Mol. Pharmacol.* **39**, 679–689.
- Puppala, D., Collis, L. P., Sun, S. Z., Bonato, V., Chen, X., Anson, B., Pletcher, M., Fermini, B., and Engle, S. J. (2013). Comparative gene expression profiling in human-induced pluripotent stem cell-derived cardiocytes and human and cynomolgus heart tissue. *Toxicol. Sci.* **131**, 292–301.
- Sedej, S., Schmidt, A., Denegri, M., Walther, S., Matovina, M., Arnstein, G., Gutsch, E.-M., Windhager, I., Ljubojević, S., Negri, S., et al. (2014). Subclinical abnormalities in sarcoplasmic reticulum Ca(2+) release promote eccentric myocardial remodeling and pump failure death in response to pressure overload. *J. Am. Coll. Cardiol.* **63**, 1569–1579.
- Selthofer-Relatic, K., Kibel, A., Delic-Brkljacic, D., and Bosnjak, I. (2019). Cardiac obesity and cardiac cachexia: Is there a pathophysiological link? *J. Obes.* **2019**, 1–7.
- Shannon, T. R., Pogwizd, S. M., and Bers, D. M. (2003). Elevated sarcoplasmic reticulum Ca<sup>2+</sup> leak in intact ventricular myocytes from rabbits in heart failure. *Circ. Res.* **93**, 592–594.
- Sinnecker, D., Laugwitz, K. L., and Moretti, A. (2014). Induced pluripotent stem cell-derived cardiomyocytes for drug development and toxicity testing. *Pharmacol. Ther.* **143**, 246–252.
- Sirenko, O., Crittenden, C., Callamaras, N., Hesley, J., Chen, Y.-W., Funes, C., Rusyn, I., Anson, B., and Cromwell, E. F. (2013a). Multiparameter in vitro assessment of compound effects on cardiomyocyte physiology using iPSC cells. *J. Biomol. Screen.* **18**, 39–53.
- Sirenko, O., Cromwell, E. F., Crittenden, C., Wignall, J. A., Wright, F. A., and Rusyn, I. (2013b). Assessment of beating parameters in human induced pluripotent stem cells enables quantitative in vitro screening for cardiotoxicity. *Toxicol. Appl. Pharmacol.* **273**, 500–507.
- Sisto, I. R., Hauck, M., and Plentz, R. D. M. (2018). Muscular atrophy in cardiovascular disease. In *Muscle Atrophy* (J. Xiao, Ed.), pp. 369–391. Springer Singapore, Singapore.
- Skinner, J. R., Winbo, A., Abrams, D., Vohra, J., and Wilde, A. A. (2019). Channelopathies that lead to sudden cardiac death: Clinical and genetic aspects. *Heart Lung Circ.* **28**, 22–30.
- Teixeira, D., Pestana, D., Santos, C., Correia-Sá, L., Marques, C., Norberto, S., Meireles, M., Faria, A., Silva, R., Faria, G., et al. (2015). Inflammatory and cardiometabolic risk on obesity: Role of environmental xenoestrogens. *J. Clin. Endocrinol. Metab.* **100**, 1792–1801.
- Truong, K. M., Cherednichenko, G., and Pessah, I. N. (2019). Interactions of dichlorodiphenyltrichloroethane (DDT) and dichlorodiphenyldichloroethylene (DDE) with skeletal muscle ryanodine receptor type 1. *Toxicol. Sci.* **170**, 509–524.
- Truong, K. M., and Pessah, I. N. (2018). Comparison of chlorantraniliprole and flubendiamide activity towards wild type and malignant hyperthermia-susceptible ryanodine receptors and heat stress intolerance. *Toxicol. Sci.* **167**, 509–523.
- Vafeiadi, M., Georgiou, V., Chalkiadaki, G., Rantakokko, P., Kiviranta, H., Karachaliou, M., Fthenou, E., Venihaki, M., Sarri, K., Vassilaki, M., et al. (2015). Association of prenatal exposure to persistent organic pollutants with obesity and cardiometabolic traits in early childhood: The rhea mother-child cohort (Crete, Greece). *Environ. Health Perspect.* **123**, 1015–1021.
- van den Berg, H., Manuweera, G., and Konradsen, F. (2017). Global trends in the production and use of DDT for control of malaria and other vector-borne diseases. *Malar. J.* **16**, 401.
- van Wyk, E., Bouwman, H., van der Bank, H., Verdoorn, G. H., and Hofmann, D. (2001). Persistent organochlorine pesticides detected in blood and tissue samples of vultures from different localities in South Africa. *Comp. Biochem. Physiol. C Toxicol. Pharmacol.* **129**, 243–264.
- Waddell, H. M. M., Zhang, J. Z., Hoeksema, K. J., McLachlan, J. J., McLay, J. C., and Jones, P. P. (2016). Oxidation of RyR2 has a

- biphasic effect on the threshold for store overload-induced calcium release. *Biophys. J.* **110**, 2386–2396.
- Wafo, E., Sarrazin, L., Diana, C., Dhermain, F., Schembri, T., Lagadec, V., Pecchia, M., and Rebouillon, P. (2005). Accumulation and distribution of organochlorines (PCBs and DDTs) in various organs of *Stenella coeruleoalba* and a *Tursiops truncatus* from Mediterranean littoral environment (France). *Sci. Total Environ.* **348**, 115–127.
- Walweel, K., and Laver, D. R. (2015). Mechanisms of SR calcium release in healthy and failing human hearts. *Biophys. Rev.* **7**, 33–41.
- Walweel, K., Molenaar, P., Imtiaz, M. S., Denniss, A., dos Remedios, C., van Helden, D. F., Dulhunty, A. F., Laver, D. R., and Beard, N. A. (2017). Ryanodine receptor modification and regulation by intracellular Ca(2+) and Mg(2+) in healthy and failing human hearts. *J. Mol. Cell. Cardiol.* **104**, 53–62.
- Watanabe, H., Honda, Y., Deguchi, J., Yamada, T., and Bando, K. (2017). Usefulness of cardiotoxicity assessment using calcium transient in human induced pluripotent stem cell-derived cardiomyocytes. *J. Toxicol. Sci.* **42**, 519–527.
- Wattigney, W. A., Irvin-Barnwell, E., Li, Z., Davis, S. I., Manente, S., Maqsood, J., Scher, D., Messing, R., Schuldt, N., Hwang, S.-A., et al. (2019). Biomonitoring programs in Michigan, Minnesota and New York to assess human exposure to Great Lakes contaminants. *Int. J. Hyg. Environ. Health* **222**, 125–135.
- Werley, C. A., Boccardo, S., Rigamonti, A., Hansson, E. M., and Cohen, A. E. (2020). Multiplexed Optical Sensors in Arrayed Islands of Cells for multimodal recordings of cellular physiology. *Nat. Commun.* **11**, 3881.
- Wescott, A. P., Jafri, M. S., Lederer, W. J., and Williams, G. S. (2016). Ryanodine receptor sensitivity governs the stability and synchrony of local calcium release during cardiac excitation-contraction coupling. *J. Mol. Cell. Cardiol.* **92**, 82–92.
- WHO (2017) Cardiovascular Disease. WHO. Available at: <https://www.who.int/cardiovascular-diseases/en/>. Accessed January 11, 2019.
- Yang, H.-T., Tweedie, D., Wang, S., Guia, A., Vinogradova, T., Bogdanov, K., Allen, P. D., Stern, M. D., Lakatta, E. G., Boheler, K. R., et al. (2002). The ryanodine receptor modulates the spontaneous beating rate of cardiomyocytes during development. *Proc. Natl. Acad. Sci. U.S.A.* **99**, 9225–9230.
- Zhang, R., and Pessah, I. N. (2017). Divergent mechanisms leading to signaling dysfunction in embryonic muscle by bisphenol A and tetrabromobisphenol A. *Mol. Pharmacol.* **91**, 428–436.
- Zhu, X., Dsikowitzky, L., Kucher, S., Ricking, M., and Schwarzbauer, J. (2019). Formation and fate of point-source non-extractable DDT-related compounds on their environmental aquatic-terrestrial pathway. *Environ. Sci. Technol.* **53**, 1305–1314.
- Zou, Y., Liang, Y., Gong, H., Zhou, N., Ma, H., Guan, A., Sun, A., Wang, P., Niu, Y., Jiang, H., et al. (2011). Ryanodine receptor type 2 is required for the development of pressure overload-induced cardiac hypertrophy. *Hypertension* **58**, 1099–1110.